Acta Crystallographica Section D
Biological Crystallography
ISSN 0907-4449

Calf spleen purine-nucleoside phosphorylase: crystal structure of the binary complex with a potent multisubstrate analogue inhibitor

Marija Luić,[a] Gertraud Koellner,[b] Tsutomu Yokomatsu,[c] Shiroshi Shibuya[c] and Agnieszka Bzowska[d]*

[a]Rudjer Bošković Institute, Bijenička 54, 10002 Zagreb, Croatia, [b]Institut für Chemie-Kristallographie, Freie Universität Berlin, Takustrasse 6, D-14195 Berlin, Germany, [c]School of Pharmacy, Tokyo University of Pharmacy and Life Science, 1432-1 Horinouchi, Hachioji, Tokyo 192-0392, Japan, and [d]Department of Biophysics, Institute of Experimental Physics, University of Warsaw, Żwirki i Wigury 93, 02 089 Warsaw, Poland

Correspondence e-mail: abzowska@biogeo.uw.edu.pl

Received 9 February 2004
Accepted 8 June 2004

PDB Reference: PNP–DFPP-G complex, 1v48, r1v48sf.

Purine-nucleoside phosphorylase (PNP) deficiency in humans leads to inhibition of the T-cell response. Potent membrane-permeable inhibitors of this enzyme are therefore considered to be potential immunosuppressive agents. The binary complex of the trimeric calf spleen phosphorylase, which is highly homologous to human PNP, with the potent ground-state analogue inhibitor 9-(5,5-difluoro-5-phosphonopentyl)-guanine (DFPP-G) was crystallized in the cubic space group $P2_13$, with unit-cell parameter $a = 93.183$ Å and one monomer per asymmetric unit. High-resolution X-ray diffraction data were collected using synchrotron radiation (EMBL Outstation, DESY, Hamburg, station X13). The crystal structure was refined to a resolution of 2.2 Å and R and $R_{\rm free}$ values of 19.1 and 24.2%, respectively. The crystal structure confirms that DFPP-G acts as a multisubstrate analogue inhibitor as it binds to both nucleoside- and phosphate-binding sites. The structure also provides the answers to some questions regarding the substrate specificity and molecular mechanism of trimeric PNPs. The wide access to the active-site pocket that was observed in the reported structure as a result of the flexibility or disorder of two loops (residues 60–65 and 251–266) strongly supports the random binding of substrates. The putative hydrogen bonds identified in the base-binding site indicate that N(1)—H and not O^6 of the purine base defines the specificity of trimeric PNPs. This is confirmed by the fact that the contact of guanine O^6 with Asn243 $O^{\delta1}$ is not a direct contact but is mediated by a water molecule. Participation of Arg84 in the binding of the phosphonate group experimentally verifies the previous suggestion [Blackburn & Kent (1986), *J. Chem. Soc. Perkin Trans. I*, pp. 913–917; Halazy *et al.* (1991), *J. Am. Chem. Soc.* **113**, 315–317] that fluorination of alkylphosphonates yields compounds with properties that suitably resemble those of phosphate esters and in turn leads to optimized interactions of such analogues with the phosphate-binding site residues. DFPP-G shows a K_i^{app} in the nanomolar range towards calf and human PNPs. To date, no high-resolution X-ray structures of these enzymes with such potent ground-state analogue inhibitors have been available in the Protein Data Bank. The present structure may thus be used in the rational structure-based design of new PNP inhibitors with potential medical applications.

1. Abbreviations

PNP, purine-nucleoside phosphorylase; DFPP-G, 9-(5,5-difluoro-5-phosphonopentyl)guanine; DPP-G, 9-(5-phosphonopentyl)guanine; HPG, 9-(hydroxypentyl)guanine; DAP, 2,8-diaminopurine; (*S*)-PMPDAP, 2,6-diamino-(*S*)-9-[2-(phosphonomethoxy)propyl]purine; N(7)-acycloguanosine, 7-[(1,3-dihydroxypropyl)-2-amino]ethylguanine; Ino, inosine; PEG, polyethylene glycol; P_i, orthophosphate; K_i^{app}, apparent

inhibition constant; K_i^*, equilibrium inhibition constant (for two-step binding exhibited by immucillin transition-state inhibitors).

2. Introduction

Purine-nucleoside phosphorylase (PNP; purine-nucleoside: orthophosphate ribosyltransferase; EC 2.4.2.1) is the key enzyme of the purine-salvage pathway (see Bzowska *et al.*, 2000). In mammals, 'low-molecular-weight' (MW $\simeq$ 90 kDa) homotrimeric PNPs catalyse the reversible phosphorolytic cleavage of the glycosidic bond of 6-oxopurine nucleosides (ribo- and 2′-deoxyribo) and some analogues as follows:

$$\text{purine nucleoside} + \text{orthophosphate} \longleftrightarrow \text{purine base} + \text{pentose-1-phosphate}. \quad (1)$$

The specificity of PNPs isolated from many prokaryotic organisms is usually not restricted to 6-oxo purine nucleosides. The genomes of some of these organisms, *e.g.* those of *Escherichia coli*, *Bacillis stearothermophilus* and *B. subtilis*, encode two distinct PNPs. The first exhibits a specificity similar to that of mammalian enzymes, while the second 'high-molecular-weight' mainly homohexameric phosphorylases (MW $\simeq$ 110–150 kDa) show broader specificity and also accept 6-aminopurine nucleoside as a substrate (see Bzowska *et al.*, 2000).

Both classes of PNPs are important targets for chemotherapy. Potent inhibitors of human and parasitic PNPs are considered to be potential chemotherapeutic agents (*e.g.* Schramm, 2002; Kicska *et al.*, 2002; see Bzowska *et al.*, 2000). The broad specificity of some prokaryotic PNPs makes them ideal candidates for gene therapy of some tumours (*e.g.* Gadi *et al.*, 2003; see Bzowska *et al.*, 2000).

In the 28 years since genetic deficiency of PNP was discovered (Giblett *et al.*, 1975), great efforts have been made to design inhibitors of PNPs with potential medical applications (see Bzowska *et al.*, 2000). However, only the transition-state analogue of human PNP, immucillin H (trade name BCX-1777), has reached phase I/II clinical trials against human T-cell leukaemia (Schramm, 2002).

The important class of potent ground-state analogue inhibitors of trimeric PNPs (K_i in the nanomolar range) is composed of so-called multisubstrate analogue inhibitors. These are compounds consisting of three structural parts linked together: (i) a purine base, (ii) an acyclic chain or cyclic moiety and (iii) a phosphonate, phosphate or other electronegative group (see Bzowska *et al.*, 2000). These three parts mimic the two substrates of PNP, namely purine nucleoside (parts 1 and 2) and phosphate (part 3) in the phosphorolytic direction or purine base and pentose-1-phosphate in the synthetic direction (see equation 1), hence they are expected to bind to purine-, pentose- and phosphate-binding sites in a binary complex with the enzyme. Complexes of trimeric PNPs with multisubstrate analogue inhibitors have been crystallized and their crystal structures have been reported (*e.g.* Guida *et al.*, 1994; Mao *et al.*, 1998). Owing to poor resolution or other reasons, however, coordinates are not available in the Protein Data Bank. In this paper, we describe for the first time the high-resolution X-ray structure of trimeric PNP with the potent (K_i^{app} = 16 and 18 nM at pH 7.4 towards calf and human enzymes, respectively; Halazy *et al.*, 1991) multisubstrate analogue inhibitor 9-(5,5-difluoro-5-phosphonopentyl)guanine (DFPP-G; see Fig. 1).

3. Experimental

3.1. Chemicals

The synthesis of the inhibitor 9-(5,5-difluoro-5-phosphonopentyl)guanine (DFPP-G) has been described elsewhere (Halazy *et al.*, 1991). Calf spleen PNP (about 30 units mg^{-1}) was obtained from Sigma and used without further purification, except that the sulfate and phosphate present in the commercial preparation were carefully removed as previously described (Bzowska, 2002; see below). Xanthine oxidase from buttermilk (1 unit mg^{-1} at 298 K), which was used in the coupled PNP assay (Stoeckler *et al.*, 1978), was also obtained from Sigma.

The PNP concentration was determined from the extinction coefficient at 280 nm for a 1% protein solution (ε_{280} = 9.6 cm^{-1}; Stoeckler *et al.*, 1978). The concentration of ligands (substrate and inhibitor) were determined spectrophotometrically from their molar extinction coefficients at pH 7: ε_{249} = 12 300 M^{-1} cm^{-1} for Ino and ε_{253} = 13 650 M^{-1} cm^{-1} for DFPP-G.

In all calculations we used the theoretical molecular weight of one monomer of the calf spleen enzyme based on its amino-

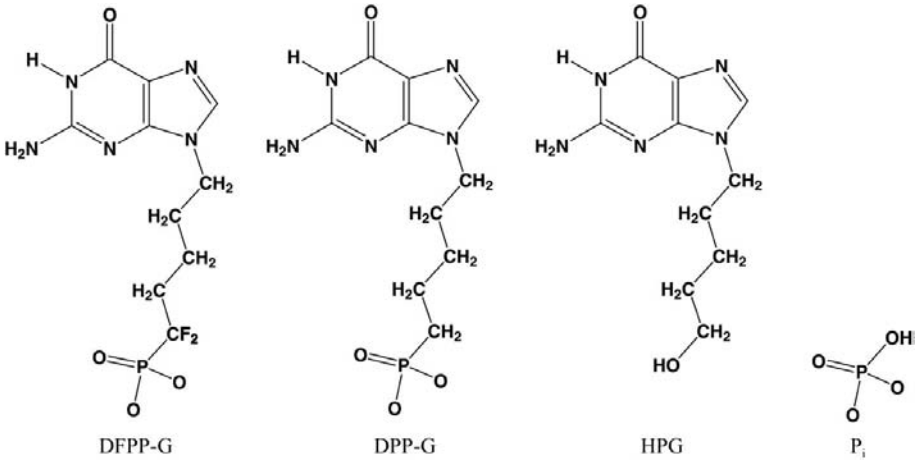

Figure 1
Structures of the multisubstrate analogue inhibitor DFPP-G and some of its precursors: non-fluorinated (DPP-G), non-fluorinated and without terminal phosphonyl group (HPG) and orthophosphate (P_i).

Table 1
Data-collection and refinement statistics for the binary complex of calf spleen PNP with 9-(5,5-difluoro-5-phosphonopentyl)guanine (DFPP-G).

Values in parentheses are for the last resolution shell (2.28–2.20 Å).

Data collection	
Space group	Cubic, $P2_13$
Unit-cell parameter (Å)	a = 93.183
Resolution (Å)	20–2.2
Total reflections	150066
Unique reflections	13902
R_{sym}†	0.055 (0.206)
$I/\sigma(I)$	25.1 (5.9)
Completeness (%)	99.7 (99.9)
Refinement statistics	
R_{factor}/R_{free} (10.2% of data) (%)	19.1/24.2
Resolution range (Å)	20.0–2.2
No. protein atoms	2034
No. inhibitor atoms	22
No. water molecules	179
No. metal atoms	2
R.m.s. deviations from stereochemical target values	
Bond lengths (Å)	0.006
Bond angles (°)	1.3
Average B values (Å^2)	
All atoms	28.0
Protein	26.9
Inhibitor	22.8
Water molecules	31.4
Mg^{2+}	18.8
Unidentified metal atom, refined as Zn^{2+}	2.0
Estimated coordinate error (after Luzzati, 1952) (Å)	0.24
Estimated coordinate error (from σ_A; Read, 1986) (Å)	0.18

† $R_{sym} = \sum|I - \langle I\rangle|/\sum I$, where $\langle I\rangle$ is the average intensity over symmetry-equivalent reflections.

acid sequence, MW = 32 093 Da (Bzowska *et al.*, 1995; Swiss-Prot accession No. P55859).

3.2. Enzyme preparation

The commercially available suspension of calf spleen PNP in ammonium sulfate was desalted and rebuffered into 20 m*M* HEPES pH 7.0 by extensive washing (at least eight times) on a Centricon YM-30 filtration device with a 30 kDa cutoff (Millipore). After desalting, the enzyme was concentrated to about 15.9 mg ml^{-1} and stored at 277 K.

The specific activity of the enzyme was determined at 298 K with 0.5 m*M* Ino and 50 m*M* phosphate buffer pH 7.0 as substrates. The spectrophotometric method was employed (λ_{obs} = 300 nm) and the phosphorolysis of Ino was coupled with the xanthine oxidase reaction (Stoeckler *et al.*, 1978). For calculation of the enzyme activity, the difference in extinction coefficients, $\Delta\varepsilon_{300\,nm}$ = 9600 M^{-1} cm^{-1}, between Ino and uric acid, the final product of the coupled reaction, was used. One unit of PNP activity is defined as 1 µmol of Ino phosphorolyzed per minute under the above conditions. The specific activity of the homogeneous and fully active calf spleen PNP is 34 units mg^{-1}.

3.3. Crystallization

The complex of the enzyme with DFPP-G was formed at pH 7.0 in 20 m*M* HEPES buffer. The final concentration of the enzyme was 8 mg ml^{-1}, while that of the ligand was 620 µ*M*.

Table 2
Inhibition of calf spleen PNP by DFPP-G, the analogue co-crystallized with calf spleen PNP in the present structure, and some of its structural precursors [non-fluorinated (DPP-G), non-fluorinated and without terminal phosphonyl group (HPG)], the binding constant for orthophosphate (P_i) and the dependence of the apparent inhibition constant (K_i^{app}) of DFPP-G on the phosphate concentration.

Analogue	Nucleoside substrate	pH	T (K)	P_i (m*M*)	K_i^{app} (n*M*)	Reference
P_i	None	7.0	298	—	∼200000†	Bzowska (2002)
HPG	Ino	7.0	298	50	>150000	Bzowska *et al.* (1991)
DPP-G	Ino	7.4	310	1.0	400 ± 80	Halazy *et al.* (1991)
DFPP-G	Ino	7.4	310	1.0	16 ± 2	Halazy *et al.* (1991)
DFPP-G	m^7Guo	7.0	298	1.0	6.9 ± 0.7	Iwanow *et al.* (2003)
DFPP-G	m^7Guo	7.0	298	0.1	2.3 ± 0.1	Iwanow *et al.* (2003)

† Binding constant.

The complex was crystallized at 291 K using the hanging-drop vapour-diffusion method: 3 µl complex solution mixed with 2 µl reservoir solution was equilibrated against 0.7 ml reservoir solution. The mother liquor used was as previously described for the crystallization with various substrates and inhibitors of other binary and ternary complexes of the calf enzyme (*e.g.* Bzowska *et al.*, 1995; Mao *et al.*, 1998; Fedorov *et al.*, 2001). The reservoir was composed of 0.1 *M* HEPES buffer pH 7.5–7.75, 0.1 *M* $MgCl_2$ and 19–31% PEG 4000.

3.4. X-ray data collection and processing

The binary complex of calf PNP with DFPP-G crystallized in the cubic space group $P2_13$, with unit-cell parameter a = 93.183 Å and one monomer per asymmetric unit (Z = 12). A complete set of X-ray diffraction data was collected at 277 K from one crystal (dome-shaped, 0.15 mm diameter) at the EMBL Outstation at DESY (Hamburg) on beamline X13 with monochromatic X-ray synchrotron radiation (λ = 0.913 Å) using a MAR Research imaging-plate detector.

Data were processed using the programs *DENZO* and *SCALEPACK* (Minor, 1993; Otwinowski, 1993). Measured intensities were converted to structure-factor amplitudes using the program *TRUNCATE* incorporated in the *CCP*4 suite (Collaborative Computational Project, Number 4, 1994). Data-collection and refinement statistics are shown in Table 1.

4. Results and discussion

4.1. Inhibitory properties of DFPP-G and its precursors

Covalent linkage of two groups, typically substrate-like moieties, both having moderate affinity for the protein leads to a more potent ligand owing to the increased effective concentration of either part when they form one molecule (*e.g.* Fersht, 1999). This is the basis for constructing multisubstrate analogue inhibitors (*e.g.* Broom, 1989). It is illustrated for calf spleen PNP in Fig. 1 and Table 2, where the structures and binding properties of the multisubstrate analogue inhibitor DFPP-G involved in the present study and some of its structural precursors are summarized. Orthophosphate and 9-(5-hydroxypentyl)guanine bind weakly to the calf enzyme (close

to the millimolar range); however, covalently joined to give 9-(5-phosphonopentyl)guanine they yield a K_i^{app} of 400 n*M* (Nakamura *et al.*, 1989) despite the lack of ether oxygen.

Since orthophosphate is one of the substrates of PNP, potent multisubstrate analogue inhibitors should carry a phosphate-like moiety in order to be able to interact effectively with the phosphate-binding site. The inhibitory properties of such analogues increase with decreasing phosphate concentration, being higher at an intracellular P_i concentration of about 1 m*M* than at the saturated 50 m*M* P_i. Unfortunately, phosphates have short plasma lifetimes owing to susceptibility to phosphatases and, because of their high negative charge, exhibit poor cellular permeability (see Montgomery, 1993). Hence, even those phosphates with dissociation constants against PNP in the nanomolar range (for example, acyclovir diphosphate shows K_i^{app} = 9 n*M* at 1 m*M* phosphate; Tuttle & Krenitsky, 1984) are not promising candidates as *in vivo* inhibitors. Replacement of phosphate by phosphonate confers metabolic stability and makes slow passage through the cell membrane possible. This leads to moderate inhibitors of PNP with K_i^{app} in the micromolar range (see Bzowska *et al.*, 2000), as previously mentioned: 9-(5-phosphonopentyl)guanine (DPP-G) has a K_i^{app} of 400 n*M* towards calf spleen enzyme. From electronic and steric considerations, Blackburn & Kent (1986) showed that α-fluoro and α,α-difluoro alkanephosphonates should better mimic phosphate esters than the corresponding phosphonates. Following this suggestion, Halazy *et al.* (1991) prepared the corresponding 9-(5,5-difluoro-5-phosphonopentyl)guanine (DFPP-G), which proved to be a more potent inhibitor, with a K_i^{app} of 16 n*M* (Table 2). The inhibitory properties of DFPP-G *versus* P_i concentration published by Iwanow *et al.* (2003) are included in Table 2. All inhibition constants shown are apparent values owing to the complex kinetic mechanism of calf spleen PNP, which leads to non-Michaelis kinetics (Bzowska, 2002). Nevertheless, data obtained under similar conditions indicate that (i) the fluorinated compound has a K_i^{app} value 25-fold lower than that of the non-fluorinated counterpart, *i.e.* 16 n*M* compared with 400 n*M*, and (ii) the apparent inhibition potency of the fluorinated compound decreases with increasing concentration of orthophosphate in agreement with the multisubstrate analogue inhibitor property of DFPP-G. The crystal structure determined in our work provides the structural basis for understanding the findings described above.

4.2. The overall structure of the enzyme

The overall structure of calf spleen PNP complexed with DFPP-G is similar to the crystal structures of various binary and ternary complexes with substrate and substrate analogues of the enzyme described previously (*e.g.* Koellner *et al.*, 1997; Mao *et al.*, 1998; Luić *et al.*, 2001; Fedorov *et al.*, 2001). The biologically active form of the enzyme is considered to be the homotrimer (Bzowska, 2002), with the active sites located at the interfaces of two monomers. The core of the enzyme subunit is a nine-stranded mixed β-barrel flanked by eight α-helices and four short 3_{10}-helices. The core carries several extended loops. One of the longest (14 amino acids) is the loop between helix H2 and β-strand S3 (see Koellner *et al.*, 1997 for notation of secondary-structure elements). Part of this loop, residues 60–65, as well as one extended loop between β-strand S9 and helix α-H10, *i.e.* residues 251–266, are not visible in the electron density in the present structure. These two regions, which are disordered or flexible in the unliganded structure in trimeric PNPs, are known to undergo independent conformational changes upon binding of substrates: residues 60–65 on binding phosphate and residues 251–266 on binding 6-oxopurines and corresponding nucleosides (Mao *et al.*, 1998; Erion *et al.*, 1997). The present crystal structure shows that the multisubstrate analogue inhibitor DFPP-G is not able to induce conformational changes similar to those caused by binding of natural substrates of the enzyme. This remains true although it carries substrate like-moieties (purine base and phosphonyl group) linked together with acyclic chain and does bind to base- and phosphate-binding sites with K_i^{app} in the 10 n*M* range.

4.3. Access to the active site and kinetic mechanism

The three active sites of the biologically active calf spleen PNP trimer are located at the interfaces of two monomers. Their surfaces comprise residues from both contacting subunits, leading to a tight pocket deeply buried in the protein structure, as shown and discussed in detail in Luić *et al.* (2001). The walls of the pocket seem to be fairly compact, but as outlined in Luić *et al.* (2001) flexibility must occur to enable binding and release of ligands in a catalytic process. The lack of electron density of two loops (residues 60–65 and 251–266) observed in the present crystal structure indicate disorder or flexibility of these two regions, despite the fact that a potent inhibitor is bound in the active site. This in turn points to both loops acting as 'swinging gates' that open and close the entrance to the active-site cavity. The active site in the present structure, with both gates not stabilized in the closed position (as observed when natural substrates are bound; Mao *et al.*, 1998; Erion *et al.*, 1997), appears to be readily accessible from the outside (Fig. 2). A 'swinging gate' consisting of residues 241–260 and controlling access to the active site was also detected in the human PNP crystal structure (Ealick *et al.*, 1991, 1992).

A sequential mechanism is well documented for trimeric PNP, but no clear agreement has been reached regarding the scenario of substrate binding: both ordered and random binding have been suggested (see Bzowska *et al.*, 2000). However, recent kinetic and binding data for calf spleen PNP (Bzowska, 2002) are consistent only with random substrate binding in the phosphorolytic direction. Accordingly, the wide access to the active-site pocket as shown in the present crystal structure of calf spleen enzyme strongly supports random binding. This is in agreement with the crystal structure of this enzyme in a new space group, in which the 'swinging gate' composed of residues 60–65 is trapped in the open conformation (Bzowska *et al.*, 2004).

4.4. Active site and specificity of the enzyme

The active site in the present crystal structure contains one molecule of DFPP-G and several water molecules. The putative hydrogen bonds in the active site are shown schematically in Fig. 2(*b*). DFPP-G binds to both base and phosphate-binding sites, proving that it acts as multisubstrate analogue inhibitor.

The phosphonyl moiety of DFPP-G is hydrogen bonded to the side chains of Ser33, Arg84, His86 and Ser220 and to Ala116 N of the backbone. These are typical contacts observed in the phosphate-binding site. However, contact with His64 is missing in the present structure, since this side chain is located in one of the 'swinging gates' leading to the active-site cavity, as described above. Each O atom of the phosphonyl moiety is linked to the protein by at least one direct hydrogen bond.

The guanine base of the inhibitor is recognized by a zigzag pattern of possible hydrogen bonds as follows: guanine N(1)$\cdots$Glu201 $O^{\varepsilon1}\cdots$guanine $NH_2\cdots$Glu201 $O^{\varepsilon2}$. The second active-site residue Asn243 $N^{\delta2}$ forms a direct contact only with N(7) of guanine (Fig. 2*b*). Similar to the pattern observed with trimeric *Cellulomonas* PNP (Tebbe *et al.*, 1999), the guanine O^6 of the inhibitor has no direct contact with the protein, but is bridged *via* a water molecule (W518) to Asn243 $O^{\delta1}$. Such a hydrogen-bonding interaction of the purine ring with the side chain of Asn243 could be formed not only for 6-oxopurines and corresponding nucleosides, but also for 6-aminopurines and its nucleosides. Based on the crystal structure of another calf spleen–inhibitor complex, this result supports the hypothesis that N(1)–H and not O^6 of the purine base defines the specificity of trimeric PNPs (Fig. 2*a*; Bzowska *et al.*, 2004).

This new hydrogen-bonding pattern observed for Asn243 indicates mobility of this active-site residue and its conformational change-induced activation: in the present structure, contact of Asn243 with purine O^6 mediated *via* a water molecule correlates well with disorder of the 'swinging gate' composed of residues 251–266.

The acyclic chain of the inhibitor is located in the ribose-binding site but makes no direct specific contacts with the protein. It seems that the main role of the chain is to link two substrate-like moieties by a flexible and sufficiently long spacer to enable optimal contact of both of them with purine and phosphate-binding sites and increase the effective concentration of these substrate-like parts (entropic effect).

An important question remains: why does fluorinated DFPP-G bind 25-fold more effectively than its non-fluorinated counterpart, 9-(5-phosphonopentyl)guanine (DPP-G)? This will be addressed in the next section.

4.5. Possible hydrogen-bonding contacts of the F atoms

F—C is a very weak hydrogen-bond acceptor. Therefore, hydrogen bonds from the strong donors O—H and N—H to organic fluorine occur only rarely in crystal structures. According to various database analyses, it is possible that between 0.6% and 3.4% of organic F atoms accept hydrogen bonds from O—H or N—H (Desiraju & Steiner, 1999). *Ab initio* calculations on O—H$\cdots$F—C hydrogen bonds yield an energy of interaction of about 10 kJ mol^{-1} in the optimal acceptor–donor distance for C(sp^3)—F hybridization (Desiraju & Steiner, 1999). Hence, if present in the DFPP-G complex with PNP, such a non-conventional hydrogen bond involving F—C could be responsible for an up to 60-fold

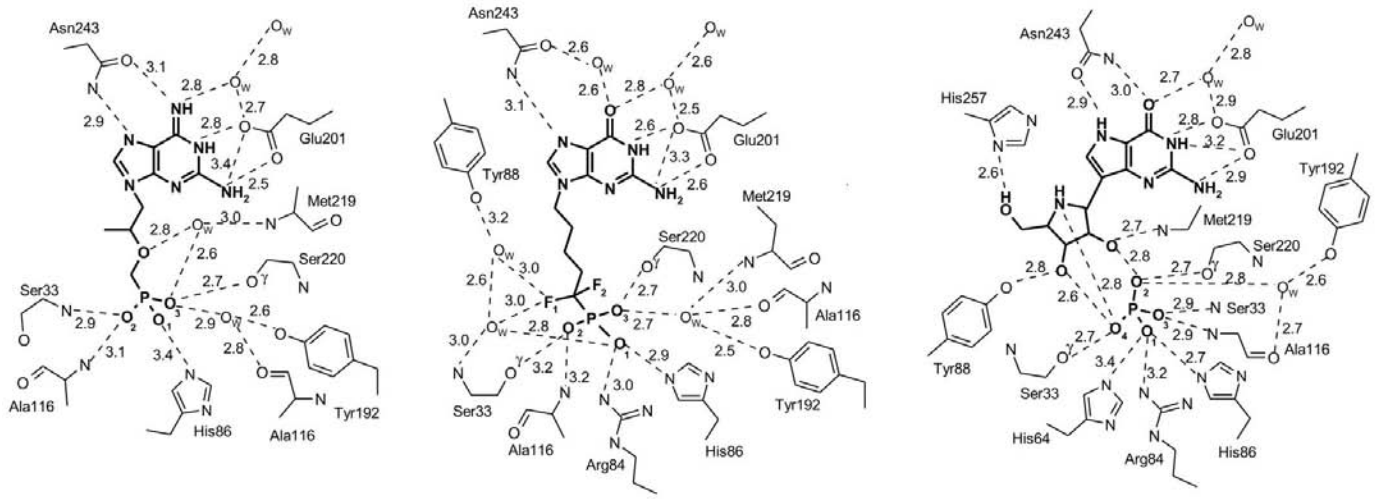

Figure 2
Modes of binding of three inhibitors in the active site of calf spleen PNP. The inhibition constants of these three analogues span almost six orders of magnitude from 30 p*M* for immucillin G to 6 μ*M* for (*S*)-PMPDAP, as shown in the figure. (*a*) Multisubstrate analogue inhibitor (*S*)-PMPDAP in a binary complex with the enzyme (PDB code 1lv8, monomer *A*; Bzowska *et al.*, 2004). (*b*) Multisubstrate analogue inhibitor DFPP-G in a binary complex with the enzyme (present structure; PDB code 1v48). (*c*) Transition-state inhibitor immucillin G in a ternary complex with the enzyme and phosphate (PDB code 1b8n; Kicska *et al.*, 2002). Possible hydrogen bonds (<3.5 Å) are indicated by broken lines. Distances are shown in Å. Inhibitory properties are from Kulikowska *et al.* (1998), Iwanow *et al.* (2003) and Miles *et al.* (1998) for (*a*), (*b*) and (*c*), respectively.

decrease of the inhibition constant as the result of the fluorination, provided that there are no other compensating factors [$\Delta\Delta G = -RT\ln(K_{d1}/K_{d2})$, where K_{d1} and K_{d2} are the dissociation constants of DPP-G and its fluorinated analogue]. This would explain the differences in affinity toward calf spleen enzyme of DPP-G, K_i^{app} = 400 n*M*, and its fluorinated analogue, DFPP-G, K_i^{app} = 16 n*M* (pH 7.4, 298 K; Halazy *et al.*, 1991).

However, in the present structure the F atoms of DFPP-G are not involved in any direct hydrogen-bonding contacts with the protein. On the other hand, indirect contacts *via* water molecules cannot be ruled out as the location of one of the F atoms, 3.0 Å away from the O atoms of two well defined water molecules (W645 and W646, see Fig. 2*b*), may indicate possible hydrogen bonds. Both water molecules could possibly be involved in direct contacts with the protein (Tyr88 O and Ser33 N), although the contribution of these interactions to the binding energy of DFPP-G cannot be regarded as unambiguous.

It seems that the more potent binding of DFPP-G relative to DPP-G is more likely to be associated with the physical characteristics of the fluorophosphonates that lead to more highly optimized interactions in the phosphate-binding site.

4.6. Effect of F atoms on the physical characteristics of the phosphonate moiety

The effectiveness of the CF_2 group as an isosteric and isoelectronic replacement for the ester oxygen in phosphomonoesters, relative to the weakly electronegative CH_2 group, is associated with three physical characteristics of fluorophosphonates. These are the acidity of the second dissociation constant, the infrared frequency of stretching of the P═O bond and the ^{31}P chemical shifts observed in NMR spectra (Blackburn & Kent, 1986). As a consequence, fluorination leads to compounds with properties resembling those of corresponding phosphate esters. This is clearly reflected in the hydrogen-bonding pattern observed in the phosphate-binding site in the present structure as compared with those reported for orthophosphate (Fig. 2*c*; Kicska *et al.*, 2002) and the phosphonate multisubstrate analogue inhibitor (*S*)-PMPDAP (Fig. 2*a*). The side chain of Arg84 forms a putative hydrogen bond with the orthophosphate and the fluorinated compound DFPP-G, while in the structure with (*S*)-PMPDAP it is directed away from the active site (Fig. 4). The free-energy contribution to the binding of a salt bridge between the positively charged Arg84 and the negatively charged phosphate-like moiety could account for the observed differ-

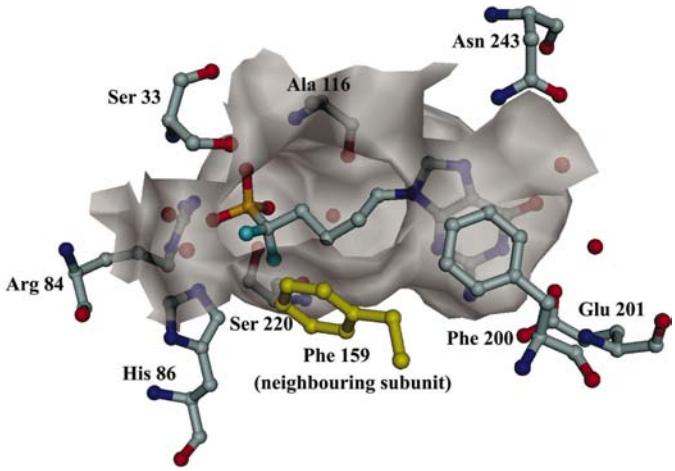

Figure 3
The binding pocket of calf spleen PNP described by means of the solvent-accessible surface calculated without the inhibitor DFPP-G (MSMS; Sanner *et al.*, 1996). The active-site amino acids that form putative hydrogen bonds with the inhibitor (see Fig. 2*b* for details) are included. Also shown is the location of Phe200, which is involved in an edge-to-face π-stacking interaction with the inhibitor base. The biologically active form of the enzyme is a homotrimer, with active sites located at the interface of two monomers. The neighbouring subunit contributes the side chain of Phe159 to the pocket (drawn in yellow). In the present structure, residues 60–65 and 251–266, *i.e.* parts of two loops, are not visible in the electron density, indicating high flexibility or disorder of these so-called 'swinging gates' leading to the active site. Owing to this phenomenon, a wide entrance into the active site is opened in the present structure. This figure was drawn with *DINO* (Philippsen, 2000).

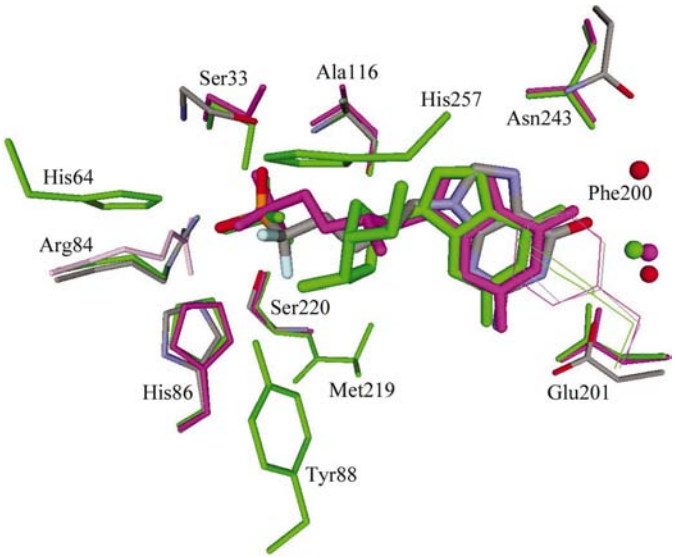

Figure 4
Superposition of the active sites of three complexes of calf spleen PNP with various inhibitors: (i) the binary complex with the multisubstrate analogue inhibitor DFPP-G (cpk colours, present structure; PDB code 1v48), (ii) the binary complex with the multisubstrate analogue inhibitor (*S*)-PMPDAP (magenta; PDB code 1lv8, monomer *A*; Bzowska *et al.*, 2004) and (iii) the ternary complex with the transition-state inhibitor immucillin G and phosphate (green; PDB code 1b8n; Kicska *et al.*, 2002). Active-site amino acids that form putative hydrogen bonds with the inhibitors are included (see also Fig. 2). In addition, the location of Phe200 involved in π-stacking interaction with the inhibitor base is also shown (thin lines). Phosphate and phosphonate groups of the multisubstrate analogue inhibitors [DFPP-G and (*S*)-PMPDAP] and orthophosphate in the ternary complex with immucillin G occupy the same position in all three structures. The side chain of Arg84 in the complex with (*S*)-PMPDAP (drawn in light magenta) is directed away from the phosphate-binding site and does not form hydrogen bonds with the phosphonate group of the inhibitor. Tyr88, Met219 and His257 only form direct hydrogen-bonding contacts in the complex with immucillin G. The inhibition potency of the three inhibitors shown in the figure spans almost six orders of magnitude: from 30 p*M* for immucillin G to 6 μ*M* for (*S*)-PMPDAP (see text for details). The number of direct hydrogen-bonding contacts formed by these three ligands correlates well with their inhibition potency as observed in solution.

ence between the K_i^{app} of DFPP-G and that of its non-fluorinated counterpart (Table 2).

4.7. Comparison with other complexes and possible use in the design of new inhibitors

DFPP-G is amongst the most potent ground-state multisubstrate analogue PNP inhibitors (K_i^{app} = 16 n*M* towards calf enzyme; Halazy *et al.*, 1991). Many such compounds show only moderate activity, *e.g.* 2,6-diamino-(*S*)-9-[2-(phosphonomethoxy)propyl]purine [(*S*)-PMPDAP; $K_i \simeq 6$ μ*M*; Kulikowska *et al.*, 1998). However, DFPP-G binds almost thousand times more weakly than immucillin G, which has been specifically designed to mimic the structure of the nucleoside substrate in the transition state (K_i^* = 30 p*M*; Miles *et al.*, 1998). The inhibition potency of these three inhibitors spans almost six orders of magnitude. Putative active-site hydrogen bonds identified in their crystal structures with calf spleen PNP (Fig. 2) correlate well with their inhibition potency. Tighter binding on going from Figs. 2(*a*) to 2(*c*) is associated with a greater total number of specific hydrogen-bond contacts and in particular with a greater number of direct contacts with the enzyme. In particular, an optimal hydrogen-bonding geometry with a flexible chain of Asn243 is possible with the hydrogen-bond donor either at N(7) of the purine base (immucillin G; Fig. 2*c*) or if such a donor is provided by a substituent placed at C(6) of the base (DAP analogue). When both sites carry hydrogen-bond acceptors, a water molecule mediates one of the contacts (Fig. 2*b*). His257, Tyr88 and Met219 only form direct contacts in the immucillin G complex. The acyclic chains of DFPP-G and (*S*)-PMPDAP occupy the pentose-binding site but are not engaged in any direct specific interactions with the enzyme, in contrast to the iminoribitol moiety of immucillin G (Figs. 2 and 3). Contacts in the phosphate-binding site are also optimized in the immucillin G complex, engaging the side chains of Arg84 and His64; the latter is missing in the DFPP-G–PNP complex, while the (*S*)-PMPDAP–PNP complex lacks both of them.

The present structure may be used to design multisubstrate analogues with optimized interactions in the base, pentose and phosphate-binding sites, eventually leading to the design of new ground-state inhibitors of PNP with potential medical applications.

We are indebted to Professor Wolfram Saenger for the possibility of carrying out the crystallographic studies in his laboratory. This project was supported by the Polish State Committee for Scientific Research (KBN 3 P04A 035 24), by Deutsche Forschungsgemeinschaft DFG (KO 1477/21 and 436 POL 17/22/98), by Scientific Research (C) from the Ministry of Education, Culture, Sports, Science and Technology of Japan, and by grant 0098036 from the Ministry of Science and Technology of the Republic of Croatia. We also acknowledge support for international collaboration in the frame of the scientific and technological cooperation between the Bundesministerium für Bildung und Forschung BMBF and the State Committee of Scientific Research (KBN) of Poland (Project Nos. POL 99-012, UM912/99 and UM991/21/2000, DZ KBN: 2539/R00/R02).

References

Blackburn, G. M. & Kent, D. E. (1986). *J. Chem. Soc. Perkin Trans. I*, pp. 913–917.
Broom, A. D. (1989). *J. Med. Chem.* **32**, 2–7.
Bzowska, A. (2002). *Biochim. Biophys. Acta*, **1596**, 293–317 (2002).
Bzowska, A., Koellner, G., Wielgus-Kutrowska, B., Stroh, A., Raszewski, G., Holý, A., Steiner, T. & Frank, J. (2004). Submitted.
Bzowska, A., Kulikowska, E. & Shugar, D. (2000). *Pharmacol. Ther.* **88**, 349–425.
Bzowska, A., Kulikowska, E., Shugar, D., Bing-yi, C., Lindborg, B. & Johansson, N. G. (1991). *Biochem. Pharmacol.* **41**, 1791–1803.
Bzowska, A., Luić, M., Schröder, W., Shugar, D., Saenger, W. & Koellner, G. (1995). *FEBS Lett.* **367**, 214–218.
Collaborative Computational Project, Number 4 (1994). *Acta Cryst.* D**50**, 760–763.
Desiraju, G. R. & Steiner, T. (1999). *The Weak Hydrogen Bond in Structural Chemistry and Biology*. Oxford University Press.
Ealick, S. E., Babu, Y. S., Bugg, C. E., Erion, M. D., Guida, W. C., Montgomery, J. A. & Secrist, J. A. III (1991). *Proc. Natl Acad. Sci. USA*, **88**, 11540–11544.
Ealick, S. E., Babu, Y. S., Bugg, C. E., Erion, M. D., Guida, W. C., Montgomery, J. A. & Secrist, J. A. III (1992). *Proc. Natl Acad. Sci. USA*, **89**, 9974.
Erion, M. D., Stoeckler, J. D., Guida, W. C., Walter, R. L. & Ealick, S. E. (1997). *Biochemistry*, **36**, 11735–11748.
Fedorov, A., Shi, W., Kicska, G., Fedorov, E., Tyler, P. C., Furneaux, R. H., Hanson, J. C., Gainsford, G. J., Larese, J. Z., Schramm, V. L. & Almo, S. C. (2001). *Biochemistry*, **40**, 853−860.
Fersht, A. (1999). *Structure and Mechanism in Protein Science: A Guide to Enzyme Catalysis and Protein Folding*. Cygnus Software Ltd.
Gadi, V. K., Alexander, S. D., Waud, W. R., Allan, P. W., Parker, W. B. & Soher, E. J. (2003). *J. Pharmacol. Exp. Ther.* **304**, 1280–1284.
Giblett, E. R., Ammann, A. J., Wara, D. W., Sandman, R. & Diamond, L. K. (1975). *Lancet*, **1**, 1010–1013.
Guida, W. C., Elliott, R. D., Thomas, H. J., Secrist, J. A. III., Babu, Y. S., Bugg, C. E., Erion, M. D., Ealick, S. E. & Montgomery, J. A. (1994). *J. Med. Chem.* **37**, 1109–1114.
Halazy, S., Ehrhard, A. & Danzin, C. (1991). *J. Am. Chem. Soc.* **113**, 315–317.
Iwanow, M., Magnowska, L., Yokomatsu, T., Shibuya, S. & Bzowska, A. (2003). *Nucleosides Nucleotides Nucleic Acids*, **22**, 1567–1570.
Kicska, G. A., Tyler, P. C., Evans, G. B., Furneaux, R. H., Schramm, V. L. & Kim, K. (2002). *J. Biol. Chem.* **277**, 3226–3231.
Koellner, G., Luić, M., Shugar, D., Saenger, W. & Bzowska, A. (1997). *J. Mol. Biol.* **265**, 202–216.
Kulikowska, E., Bzowska, A., Holý, A., Magnowska, L. & Shugar, D. (1998). *Adv. Exp. Med. Biol.* **431**, 747–752.
Luić, M., Koellner, G., Shugar, D., Saenger, W. & Bzowska, A. (2001). *Acta Cryst.* D**57**, 30–36.
Luzzati, V. (1952). *Acta Cryst.* **5**, 802–810.
Mao, C., Cook, W. J., Zhou, M., Fedorov, A. A., Almo, S. C. & Ealick, S. E. (1998). *Biochemistry*, **37**, 7135–7146.
Miles, R. W., Tyler, P. C., Furneaux, R. H., Bagdassarian, C. K. & Schramm, V. L. (1998). *Biochemistry*, **37**, 8615–8621.
Minor, W. (1993). *XDISPLAYF Program*. Purdue University, West Lafeyette, IN, USA.
Montgomery, J. A. (1993). *Med. Res. Rev.* **13**, 209–228.
Nakamura, C. E., Chu, S.-H., Stoeckler, J. D. & Parks, R. E. Jr (1989). *Nucleosides Nucleotides*, **8**, 1039–1040.
Otwinowski, Z. (1993). *Proceedings of the CCP4 Study Weekend. Data Collection and Processing*, edited by L. Sawyer, N. Isaacs & S. Bailey, pp. 56–62. Warrington: Daresbury Laboratory.

Philippsen, A. (2000). *DINO: Visualizing Structural Biology*, http://www.biozentrum.unibas.ch/~xray/dino.
Read, R. J. (1986). *Acta Cryst.* A**42**, 140–149.
Sanner, M. F., Spehner, J.-C. & Olson, A. J. (1996). *Biopolymers*, **38**, 305–320.
Schramm, V. L. (2002). *Biochim. Biophys. Acta*, **1587**, 107–117.
Stoeckler, J. D., Agarwal, R. P., Agarwal, K. C. & Parks, R. E. Jr (1978). *Methods Enzymol.* **51**, 530–538.
Tebbe, J., Bzowska, A., Wielgus-Kutrowska, B., Kazimierczuk, Z., Schröder, W., Shugar, D., Saenger, W. & Koellner, G. (1999). *J. Mol. Biol.* **294**, 1239–1255.
Tuttle, J. V. & Krenitsky, T. A. (1984). *J. Biol. Chem.* **259**, 4065–4069.